eNAMPT/TLR4 inflammatory cascade activation is a key contributor to SLE Lung vasculitis and alveolar hemorrhage

Gantsetseg Tumurkhuu [a,b], Nancy G. Casanova [d], Carrie L. Kempf [d], Duygu Ercan Laguna [a,b], Sara M. Camp [d], Jargalsaikhan Dagvadorj [b], Jin H. Song [d], Vivian Reyes Hernon [d], Cristina Travelli [e], Erica N. Montano [a,b], Jeong Min Yu [a], Mariko Ishimori [a,c], Daniel J. Wallace [a,c], Saad Sammani [d], Caroline Jefferies [a,b], Joe G.N. Garcia [d,*]

[a] Department of Medicine, Division of Rheumatology, Cedars-Sinai Medical Center, Los Angeles, CA, USA
[b] Department of Biomedical Sciences, Cedars-Sinai Medical Center, Los Angeles, CA, USA
[c] David Geffen School of Medicine at University of California Los Angeles (UCLA), Los Angeles, CA, USA
[d] Department of Medicine, University of Arizona Health Sciences, Tucson, AZ, USA
[e] University of Pavia, Pavia, Italy

ARTICLE INFO

ABSTRACT

Rationale: Effective therapies to reduce the severity and high mortality of pulmonary vasculitis and diffuse alveolar hemorrhage (DAH) in patients with systemic lupus erythematosus (SLE) is a serious unmet need. We explored whether biologic neutralization of eNAMPT (extracellular nicotinamide phosphoribosyl-transferase), a novel DAMP and Toll-like receptor 4 ligand, represents a viable therapeutic strategy in lupus vasculitis.

Methods: Serum was collected from SLE subjects (n = 37) for eNAMPT protein measurements. In the preclinical pristane-induced murine model of lung vasculitis/hemorrhage, C57BL/6 J mice (n = 5–10/group) were treated with PBS, IgG (1 mg/kg), or the eNAMPT-neutralizing ALT-100 mAb (1 mg/kg, IP or subcutaneously (SQ). Lung injury evaluation (Day 10) included histology/immuno-histochemistry, BAL protein/cellularity, tissue biochemistry, RNA sequencing, and plasma biomarker assessment.

Results: SLE subjects showed highly significant increases in blood *NAMPT* mRNA expression and eNAMPT protein levels compared to healthy controls. Preclinical pristane-exposed mice studies showed significantly increased NAMPT lung tissue expression and increased plasma eNAMPT levels accompanied by marked increases in alveolar hemorrhage and lung inflammation (BAL protein, PMNs, activated monocytes). In contrast, ALT-100 mAb-treated mice showed significant attenuation of inflammatory lung injury, alveolar hemorrhage, BAL protein, tissue leukocytes, and plasma inflammatory cytokines (eNAMPT, IL-6, IL-8). Lung RNA sequencing showed pristane-induced activation of inflammatory genes/pathways including NFkB, cytokine/chemokine, IL-1β, and MMP signaling pathways, each rectified in ALT-100 mAb-treated mice.

Conclusions: These findings highlight the role of eNAMPT/TLR4-mediated inflammatory signaling in the pathobiology of SLE pulmonary vasculitis and alveolar hemorrhage. Biologic neutralization of this novel DAMP appears to serve as a viable strategy to reduce the severity of SLE lung vasculitis.

1. Introduction

SLE is a systemic autoimmune disease with multiorgan involvement and an unpredictable relapsing-remitting course which disproportionately affects women, with African American and Hispanic populations having higher mortality risk [1]. SLE vasculitis is a common manifestation of SLE involving the skin, kidney and lung. Although the exact prevalence of lung involvement in SLE is unknown, many SLE patients exhibit signs of respiratory and pulmonary vascular involvement including vasculitis and diffuse alveolar hemorrhage (DAH) [2–5]. DAH as an acute form of SLE vasculitis (5–10% of patients) represents a catastrophic SLE complication with a 35–50% mortality rate for which current treatments are extremely limited [6–9]. Corticosteroids and immunosuppressive agents, such as methotrexate and

cyclophosphamide, and mechanical ventilation remain primary treatments in management of acute immune-mediated lung vasculitis/hemorrhage with subsequent respiratory failure [10]. There remains a serious unmet need for increased understanding of acute SLE lung pathophysiology and for novel effective therapeutics.

Current concepts of SLE vasculitis have highlighted key involvement of dysregulated inflammatory cascades which adversely affect the lung vasculature in SLE. Activation of these evolutionarily-conserved inflammatory pathways presumably occurs via cell-, immune complex-, or autoantibody-mediated mechanisms and/or danger-associated molecular pattern (DAMP) proteins released from injured tissues that bind to pathogen recognition receptors. In addition to SLE, DAMPs have been implicated in autoimmune disorders such as psoriasis, rheumatoid arthritis, and inflammatory bowel disease [11]. In the present study, we explored the potential contribution of the novel DAMP and TLR4 ligand, eNAMPT (extracellular nicotinamide phosphoribosyl-transferase), as a viable therapeutic target in human and preclinical SLE vasculitis. eNAMPT binding to the pathogen-recognition receptor, TLR4 [12] elicits profound NFκB-mediated inflammatory cytokine release and increases vascular permeability [13,14], events implicated in acute human inflammatory lung disorders such as ARDS [15,16] and chronic inflammatory conditions including radiation-induced pneumonitis (27) and fibrosis (39). Plasma eNAMPT levels serve as a novel biomarker in ARDS and pulmonary hypertension [17,18], and *NAMPT* promoter SNPs confer increased risk of inflammatory disease severity [17,19–23]. Importantly, studies utilizing conditionally-engineered, endothelial cell (EC)-specific *NAMPT* KO mice, provided compelling support for eNAMPT expression and secretion from vascular endothelial cells as a major driver of acute inflammatory lung injury severity [24] and vascular remodeling in PH [25].

We utilized human SLE blood samples and the murine model of pristane-induced lung vasculitis and DAH to address the participation of eNAMPT/TLR4 signaling in acute autoimmune vascular inflammation and injury. Intraperitoneal (IP) injection of pristane (TMPD, 2, 6, 10, 14-tetramethylpentadecane), a hydrocarbon oil, produces substantial alveolar and perivascular inflammation (capillaritis, small vessel vasculitis), hemorrhage, endothelial cell injury, and infiltration of macrophages, neutrophils, and proinflammatory cytokines over the ensuing 10 days [5,26]. The development of lung damage in the pristane murine model appears relevant to human lupus pulmonary vasculitis as it implicates prominent roles for innate immunity -induced inflammation with heavy monocyte and neutrophil involvement in driving the autoimmune lung pathology [5,27].

Our data indicate that eNAMPT expression is increased in human SLE subjects and pristane-challenged mice with vasculitis. Administration of an eNAMPT-neutralizing humanized mAb significantly reduces the severity of murine pristane-induced vasculitis and alveolar hemorrhage suggesting a potentially novel therapeutic target and biologic intervention for SLE-associated vasculitis and DAH.

2. Materials and methods

2.1. Reagents

The p-NFκB, NFκB, and DOCK1 antibodies were purchased from Cell Signaling Technologies (Danvers, MA); NAMPT antibody from Bethyl Laboratories (Montgomery, TX); β-actin antibody from Sigma-Aldrich (St. Louis, MO); and rabbit secondary antibody from Jackson ImmunoResearch (West Grove, PA), All other reagents were from Sigma-Aldrich. Details of the generation of the eNAMPT-neutralizing humanized mAb, ALT-100 (provided by Aqualung Therapeutics Corporation, Tucson, AZ) have been previously described [28,29].

2.2. Human SLE subjects

Peripheral blood samples from SLE patients (meeting ACR classification criteria for SLE) and healthy controls (HC) (age and sex-matched) were collected via a protocol approved by the local institutional review board. All participants provided informed written consent and the study received prior approval from the institutional ethics review board (IRB protocol #19627). Inclusion included all male and female SLE patients, >18 years of age who meet revised ACR Criteria for SLE [30]. There were no exclusion criteria as all SLE subjects were part of the repository.

2.3. Mouse pristane model

All animal protocols were approved by the fully accredited Institutional Animal Care and Use Committees of the University of Arizona and Cedars Sinai Medical Center and all experiments were performed in compliance with ARRIVE guidelines. Four series of experiments were conducted in wild-type female C57BL/6 mice (6–8 weeks old) with each series consisting of one group of unexposed controls and 3 or 4 groups of mice which were exposed to a single IP injection of 0.5 mL of pristane (2,6,10,14-Tetramethylpentadecane (TMPD), Sigma). In two series of experiments, pristane-exposed mice received either intraperitoneal PBS, isotype IgG control Ab (1 mg/kg), or the eNAMPT-neutralizing humanized mAb, ALT-100 (1 mg/kg) on days 1 and 7 (n = 9 per group). In two additional series of experiments, pristane-challenged mice received either subcutaneously delivered PBS, or 0.4 mg/kg, 1 mg/kg, 4 mg/kg ALT-100 mAb. Mice in each series of experiments were sacrificed at Day 10 post pristane.

2.4. Bronchoalveolar lavage (BAL) analysis

BAL fluid and cells were collected by lavage and centrifuged as described previously for mice [24,31]. BAL albumin and total protein and cell count analysis were performed as we previously described [32].

2.5. Quantitative lung histology and immunohistochemistry (IHC) analyses

Lungs were fixed overnight in 10% buffered formalin and embedded in paraffin. The embedded tissue was sectioned for routine hematoxylin and eosin staining and imaging (Olympus digital camera, 10x magnification) [33]. For IHC visualization of NAMPT expression in lung tissues, the avidin-biotin-peroxidase method was utilized with a rabbit anti-human NAMPT pAb (1:100 dilution, Bethyl Laboratories) as previously described [12,34,35]. Histological and IHC images were randomly selected for H&E or NAMPT quantification using ImageJ software [36] with additional details provided in the Supplemental Materials and Methods. AF647-conjugated secondary antibodies against rabbit IgG were applied at a dilution of 1:500 for 1 h at room temperature. Secondary antibody given alone without primary antibody was used as negative control for each stain.

2.6. Plasma/serum measurements of human and murine cytokines

Human serum samples were analyzed for levels of eNAMPT, IL-6, Angiopoietin-2 and IL-1RA utilizing a meso-scale ELISA platform (Meso Scale Diagnostics, Rockville, MD) as previously reported [20,37]. Similarly, murine plasma levels of eNAMPT, IL-6, and IL-8 (KC) were measured using the U-Plex MSD platform as we have previously described [23,24,38].

2.7. Flow cytometry

The following conjugated anti-mouse antibodies were used for flow cytometry studies: anti-Ly6G (1A8), anti-CD11b (M1/70), anti-Ly6C (ER-MP20), anti-F4/80 (BM8), anti-CD4 (GK1.5), anti-CD8a (53–6.7), anti-CD11c (3.9), and anti-B220 (RA3-6B2) (eBiosciences). Cells were incubated in CD16/32 (Fc block; BD Biosciences) prior to staining. Cells

were acquired on LSR II (BD Biosciences) and analyzed with the FlowJo software (Treestar).

2.8. Biochemical studies

Western blotting of lung homogenates was performed according to standard protocols as previously reported [17,32] with densitometric quantification of lung tissue expression of p-NFκB, NFκB, NAMPT, DOCK1 and β-actin (total protein control).

2.9. Gene expression analysis by Q-PCR

RNA was isolated from SLE subjects and from murine lung tissues and Quantitative PCR (Q-PCR) performed as described previously [38]. In brief, total RNA was extracted from lung using TRIzol reagent (Invitrogen, Carlsbad, CA). RNA was isolated from human blood with the QIAamp RNA Blood Mini Kit (Qiagen). cDNA was synthesized using the Superscript II First-Strand Synthesis kit (Invitrogen). SYBR Green Q-PCR analysis was performed using an Q5 (Applied systems). Gene expression was normalized to 18 S RNA, and the expression level was calculated using the 2-ΔΔCt method. Primer sequences are listed as follows: m*Nampt* Fw: tgtgtaccgaggagacgaca; m*Nampt* Rv: ctgtgccaggctgacatcta; mGapdh Fw: catcaagaaggtggtgaagc; mGapdh Rv: cctgttgctgtagctgtatt; h*NAMPT* Fw: CACACTGGA GTGGTGTACTAGC; h*NAMPT* Rv: CCAGGGTAACATCTAGCTGGAA; 18S Fw: GCTTA ATTTGACTCAA-CACGGGA; 18S Rv: AGCTATCAATCTGTCAATCCTGTC.

2.10. RNA sequencing and Gene expression analysis

Total RNA was extracted from mice lung tissues, quantified (Qubit fluorometer, ThermoFisher Scientific, Waltham, MA), and the RNA quality assessed using the 2100 Bioanalyzer (Agilent Technologies, Santa Clara, CA). RNA was purified using the NEBNext® Poly(A) mRNA Magnetic Isolation Module (New England Biolab Inc, Ipswich, MA), and library construction was performed using the Swift RNA Library Kit (Swift Biosciences, Ann Arbor, MI). Libraries were multiplexed and sequenced using NovaSeq 6000 (Illumina, San Diego, CA).

For data analysis, the raw data was converted to fasq format, reads aligned to the transcriptome using STAR (version 2.6.1) [39] and quantified using RSEM [40], a custom mouse GRCm38 transcriptome. DEseq2 [41] algorithms were used to assess the differential expression between two sample groups and a false discovery rate (FDR) [42] applied to control for multiple testing error. Enriched analysis was conducted applying Gene Ontology (GO) classification, focused on biological process and pathway classification for the statistically-significant DEGs. Unbiased comparison of the gene sets to ConsensusPathDB [43] against KEGG and Reactome pathways databases was conducted as previously reported [23,25,38]. The STRING database was used to construct the interaction networks [44].

2.11. Lung pathological evaluation

The presence of alveolar hemorrhage in lung specimens was initially assessed by gross observation of excised lungs. The percentage of lung involved with hemorrhage was assessed and a DAH score generated in a blinded manner as follows: (0) - lung hemorrhage absent; (1) 0–25% hemorrhagic lung; (2) 25–50% hemorrhagic lung; (3) 50–75% hemorrhagic lung; (4) 75–100% hemorrhagic lung.

2.12. Statistical methods

All data are expressed as means ± SD. Statistical differences were measured using either an unpaired Student's *t*-test or 2-way analysis of variance (ANOVA) when appropriate with Bonferroni *post-hoc* test. When the data analyzed was not distributed normally, we used the Mann–Whitney test or Kruskal–Wallis 1-way ANOVA with Dunn's *post-*

hoc test. Data analysis was performed using Prism software version 7.0a (GraphPad, San Diego, CA). A *P*-value of <0.05 was considered statistically significant. Asterisks in the figures represent the following: *$P <$ 0.05; **$P < 0.01$; ***$P < 0.001$, and ****$P < 0.0001$. eNAMPT levels were correlated with clinical indices by Pearson correlation.

3. Results

3.1. Increased NAMPT mRNA and protein expression in blood from SLE subjects

NAMPT mRNA expression was assessed by RT-PCR in whole blood obtained from 38 healthy controls (HCs) and 41 SLE patients (39 female, 2 male) with a mean age of 39 ± 12 years and a mean SLEDAI score of 4.7 ± 4.2 (Table 1). The SLE cohort showed a near 4-fold increase in *NAMPT* mRNA expression compared to controls (Fig. 1A). Examination of serum levels of eNAMPT, IL-6, IL-8, IL-1RA and ANG-2 from the same SLE cohort revealed that only eNAMPT levels were significantly elevated in SLE subjects when compared to healthy controls (Fig. 1B) with IL-6, IL-8, IL-1RA and ANG-2 levels in SLE subjects comparable to healthy controls (Fig. 1C/D/E/F). We assessed the relationship between eNAMPT mRNA and protein expression levels in blood and the Systemic Lupus Erythematosus Disease Activity Index or SLEDAI. Whereas eNAMPT mRNA expression levels did not show significant correlation with SLEDAI scores (p = 0.2), In contrast, plasma eNAMPT levels strongly trended to a significant relationship between plasma eNAMPT levels and SLEDAI (0.06).

3.2. Increased NAMPT mRNA and protein expression in lung tissues and blood from pristane-exposed mice with pulmonary vasculitis/hemorrhage

We next examined *Nampt* mRNA and eNAMPT plasma levels in our preclinical model of pristane-induced SLE vasculitis. Initial studies to determine the level of NAMPT expression in pristane-exposed lung tissues revealed significantly *Nampt* mRNA expression (~3-fold increase) compared to non-pristane-exposed control mouse lungs (Fig. 2A). In addition, Day 10 plasma eNAMPT levels were significantly elevated in pristane-exposed, IgG isotype antibody-treated mice (1.55± 0.3 ng/mL, n = 9) compared to non-pristane-exposed, IgG-treated controls (1.01 ± 0.2 ng/mL, n = 9, p < 0.05) (Fig. 2C). NAMPT protein expression in pristane-exposed lung tissues assessed by IHC on day 10 demonstrated

Table 1
Clinical information on a human SLE cohort (n = 41).

|	Mean ± S.D.	Median (Min-Max)
Age	39 ± 12 years	44 (20–68)
Sex Female: Male	39 : 2	
SLEDAI	4.7 ± 4.2	4 (0–18)
Organ Involvement		
Skin Involvement	5	
Arthritis	14	
Kidney	4	
Lupus Headache	1	
Low Complement	3	
Mucosal Ulcers	1	
Vasculitis	2	
Unknown	1	
Lab Work	**[Ref. Range]**	
Serum Creatinine mg/dL	0.7 ± 0.2 [0.59–1.04]	0.6 (0.5–1.3)
Serum Protein g/dL	7.1 ±0.7 [6–8]	7.1 (5.9–8.9)
Urine Creatinine	61.9 ± 42.5	46 (20.4–122.1)
C3 mg/dL	102.4 ± 36.3 [80–160]	97 (42–179.7)
C4 mg/dL	22.2 ± 12 [15–45]	18 (5–60)
ESR mm/hr	34.2 ± 21.5 [0–29]	29 (3–72)
CRP mg/dL	4 ± 4.2 [<1]*	1 (0.3–15.5)
Medications		
Antimalarials	58%	
Steroids (2.5–20 mg)	58%	
Immunosuppressants	33%	
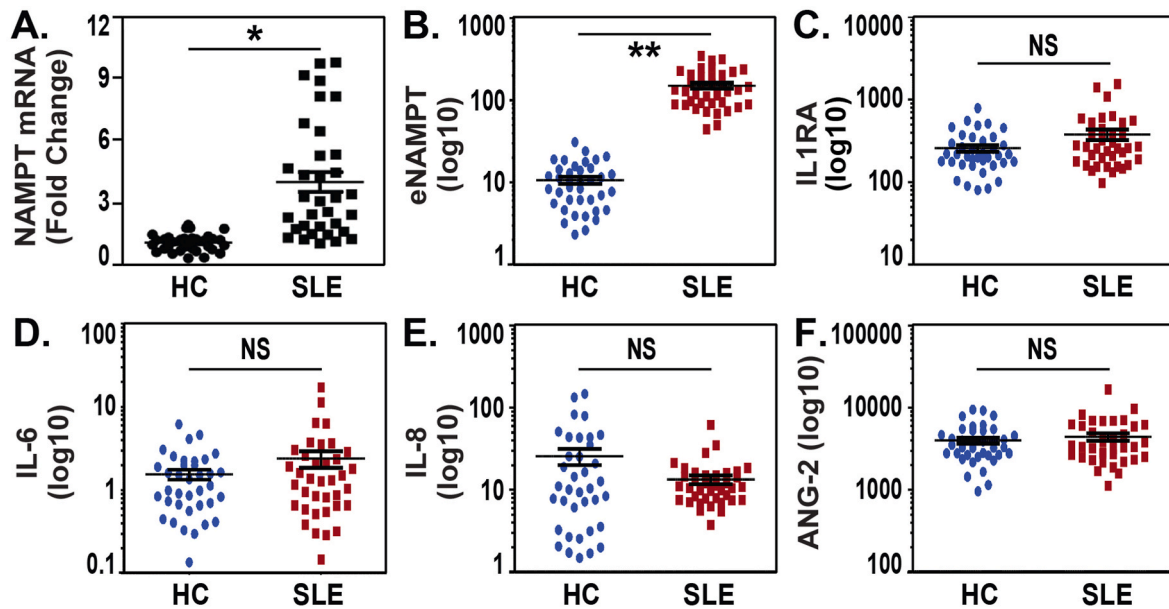
Fig. 1. Increased NAMPT expression in blood from SLE subjects. A. Whole blood was obtained from 38 healthy controls (HCs) and 41 SLE patients (>90% female) (Table 1). *NAMPT* mRNA expression was assessed by RT-PCR with >4 fold increase in *NAMPT* mRNA expression observed in SLE subjects compared to HCs. RT-PCR analysis was performed in duplicates and analyzed using ddCt method. *p < 0.01. **B/C/D/E/F.** Examination of circulating serum levels of eNAMPT, IL-6, IL-8, IL-1RA and ANG2 in 41 SLE subjects revealed that only eNAMPT levels were significantly elevated in SLE subjects compared with 38 HCs with serum levels of IL-6, IL-8, IL-1RA and ANG2 similar to HCs. All data represent mean ± SD. Statistical significance was determined using two tails Student's t-test. **p < 0.001.

significant increases in NAMPT lung tissue protein expression with steady increases in NAMPT expression from Day 1 through Days 7 and 10 (Fig. 2C). Finally, confirming the IHC imaging results, increases in NAMPT expression in pristane-exposed lung homogenates were identified by western blotting (Fig. 2D/E). Taken together, these data suggest that eNAMPT expression is markedly increased in the blood and serum of SLE patients and in the lungs and blood of pristane-challenged mice, a preclinical model of SLE lung vasculitis/hemorrhage.

3.3. The eNAMPT-neutralizing mAb reduces pristane-induced murine alveolar hemorrhage

We next assessed whether tissue and blood eNAMPT expression is an active participant in pristane-induced vasculitis/DAH and tested the effects of the ALT-100 mAb eNAMPT-neutralizing antibody in the pristane model (28, 61). Alveolar hemorrhage was absent in control mice that were not exposed to pristane challenge whereas all pristane-exposed mice receiving either PBS or IgG (controls) survived to Day 10 exhibited varying degrees of alveolar hemorrhage (mild to severe) by gross whole lung pathology (Fig. 3A/B). Quantification of the extent of lung involvement with alveolar hemorrhage demonstrated similar severity in both the PBS- and IgG-treated pristane-challenged groups with each groups exhibiting comparable (30%) incidence of mild DAH and severe DAH (Fig. 3C). In contrast, mice receiving the eNAMPT-neutralizing ALT-100 mAb (1 mg/kg, IP) beginning on Day 1 showed substantial reduction in the severity of DAH by gross examination (Fig. 3A/B) and only 10% of mAb-treated mice exhibiting severe lung hemorrhage involvement compared to 30% lung hemorrhage involvement in PBS or IgG-challenged mice (Fig. 3C). Histologic examination of pristane-induced lung inflammatory injury by H&E staining revealed dramatic immune cell and leukocyte infiltration in perivascular area which was similar in both PBS- and IgG-treated mice but significantly reduced in mice treated with the ALT-100 mAb (Fig. 3D), verified by Image J quantification of randomly selected H&E areas (Fig. 3E).

In selected experiments, the efficacy of subcutaneously-delivered ALT-100 mAb (delivered in Day 1 and Day 8) at doses of 0.4 mg/kg, 1 mg/kg, and 4 mg/kg was tested in pristane-exposed mice. Each subQ-

delivered ALT-100 mAb dose strongly reduced BAL inflammatory cell numbers with only 1 mg/kg and 4 mg/kg ALT-100 mAb significantly reducing BAL protein levels (Supplemental Fig. 1A/B). Each dose also reduced inflammatory edema and alveolar hemorrhage (1 mg/kg shown in Supplemental Fig. 1C).

3.4. eNAMPT neutralization reduces pristane-induced murine lung inflammation

Pristane-exposed mice exhibited significant inflammatory injury reflected by several BAL, tissue and blood indices. For example, BAL protein levels and numbers of BAL inflammatory cells at Day 10 were significantly increased in pristane-exposed, IgG-treated mice compared to unexposed controls (Fig. 4A/B) but significantly reduced in mice receiving the ALT-100 mAb (Fig. 4A/B). In contrast, quantification of peritoneal lavage cells from pristane-challenged mice showed no significant effect of ALT-100 mAb compared to IgG control mice (Fig. 4C). These observations indicate that treatment with the eNAMPT-neutralizing ALT-100 mAb attenuates pristane-induced lung vasculitis with reductions in vascular leak, inflammatory cell influx, NAMPT tissue expression (Fig. 2D/E) and production of proinflammatory cytokines with significant reductions in plasma levels of eNAMPT (Fig. 2B), IL-6 and IL-8 (Fig. 4D/E).

We further examined inflammatory cell subsets in pristane-exposed lungs by flow cytometry [45,46] and observed significant accumulation of Siglec 1-positive CD11b + Ly6C + monocytes in the lung (Fig. 4F), whereas CD45−CD31+ vascular endothelial cells were significantly reduced by pristane exposure (Fig. 4G). ALT-100 mAb-treated mice showed normalization of these cellular inflammatory parameters with reduced numbers of Siglec1-positive CD11b + Ly6C + monocytes and increased numbers of lung endothelial cells compared to pristane only or IgG-treated mice (Fig. 4F/G).

3.5. eNAMPT neutralization reduces pristane-induced inflammatory signaling and differentially-expressed genes/pathways

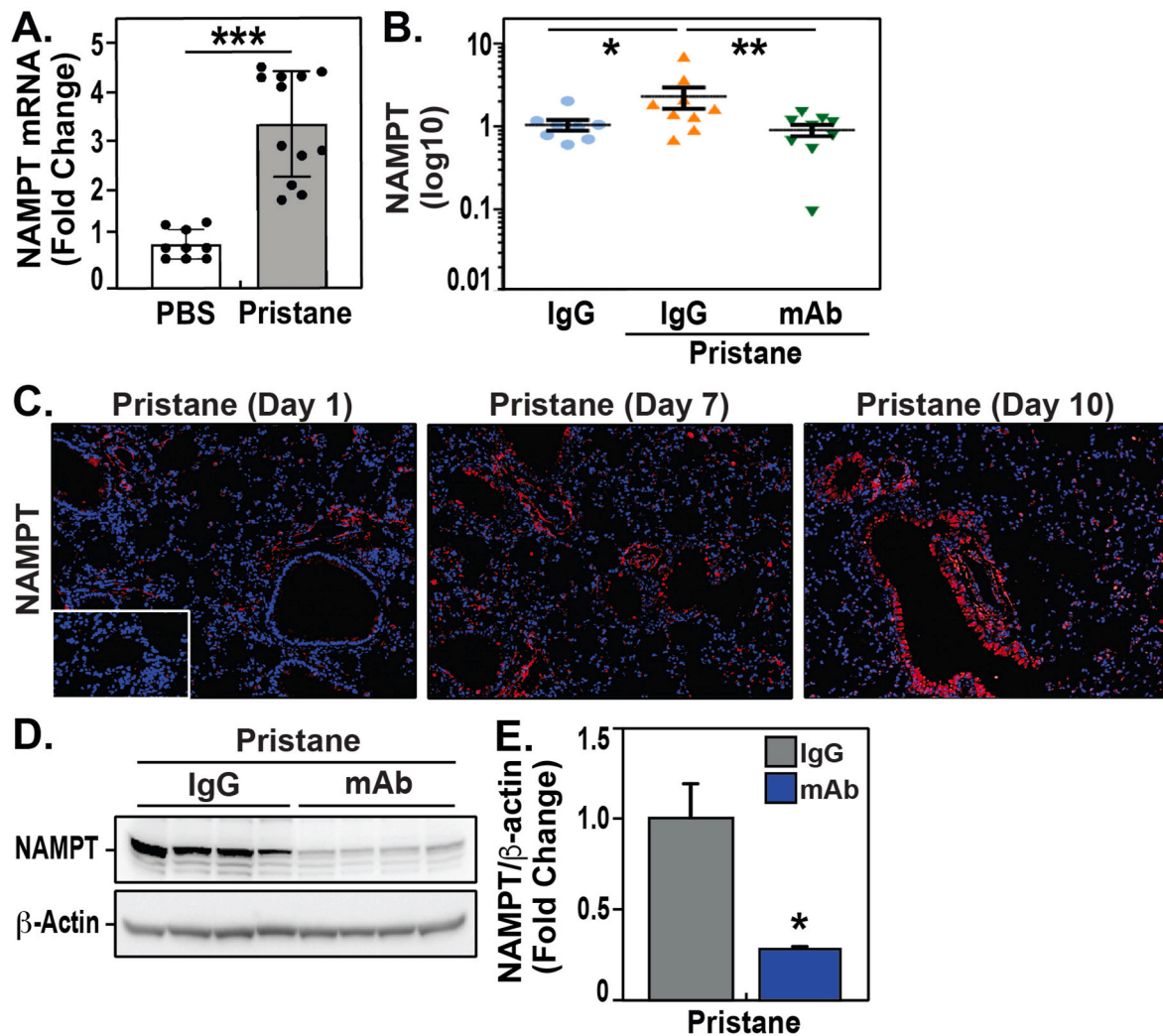To confirm that eNAMPT/TLR4 signaling contributes to lung

Fig. 2. Increased NAMPT mRNA and protein expression in lung tissues and blood from pristane-exposed mice with pulmonary vasculitis/hemorrhage. A. The level of Nampt mRNA expression in pristane-exposed murine lung tissues was examined by RT-PCR. These studies revealed significantly increased *Nampt* mRNA expression (~3-fold increase) compared to control, pristane-unexposed mouse lungs. **B.** Day 10 plasma levels of eNAMPT from IgG- and pristane-exposed mice (n = 9 samples/group). A 3-fold increase in eNAMPT levels was observed in pristane-exposed, IgG-treated mice (1.55± 0.3 ng/mL, n = 9) compared to non-pristane-exposed controls (1.01 ± 0.2 ng/mL, n = 9, p < 0.05). Mice receiving the ALT-100 eNAMPT mAb on Day 1 (1 mg/kg) demonstrated significantly reduced plasma eNAMPT levels. **C.** NAMPT protein expression in pristane-exposed lung tissues was assessed by IHC on Day 10 (Bethyl Ab, 1:1000 dilution). These studies demonstrated significant increases in NAMPT lung tissue protein expression with steady increases in NAMPT expression from Day 1 through Days 7 and 10. **D/E.** NAMPT protein expression in pristane-exposed lung homogenates, assessed via western blotting (Bethyl Ab, 1:1000 dilution), showed NAMPT lung tissue expression is markedly increased by pristane challenge and attenuated in mice receiving the eNAMPT-neutralizing ALT-100 mAb. Densitometric analysis was performed using Bio-Rad Image Lab 6.01 software to quantify protein expression normalized to b-actin expression.

inflammation, vasculitis and DAH, we performed biochemical and genomic analyses of pristane-exposed lung tissues. Striking increases in the levels of phosphorylated NFκB (standardized against total NFκB) were observed in lung homogenates obtained from pristane-exposed mice being identified by Western blotting (Fig. 5A/B) reflecting strong activation of innate immunity-mediated activation of inflammatory signaling pathways. Importantly, mice receiving the eNAMPT-neutralizing ALT-100 mAb demonstrated near abolishment of the increased levels of phosphorylated NFκB in pristane-exposed mice indicating that the eNAMPT/TLR4 inflammatory signaling pathways is a major driver of the innate immunity response to pristane challenge (Fig. 5A/B). We recently identified the Dock1 protein as a critical regulator of vascular barrier integrity via its requirement for activation of Rac GTPase-mediated cytoskeletal protein rearrangement in vascular endothelial cells [47] with TLR4 activation resulting in marked decreases in Dock1 expression. Western blot analysis of pristane-exposed lung tissue homogenates identified significant reductions in DOCK1

lung expression, which were preserved in mice receiving the eNAMPT-neutralizing ALT-100 mAb (Fig. 5A/C), thus directly linking eNAMPT/TLR4-mediated reductions in DOCK1 to a signaling pathway involved in maintaining vascular barrier integrity.

We also analyzed RNA sequencing data from pristane-exposed lung tissues to further validate the histologic and biochemical findings implicating eNAMPT/TLR4 inflammatory cascade signaling as the mechanism of action for ALT-100 mAb efficacy in pristane-induced lung vascular injury. Analyses of differentially-expressed genes (DEGs) between control mice and pristane-exposed lung tissues (Day 10) identified 604 DEGs (FDR 0.05, FC 2.0) with Gene Ontologies (GO) that were associated with inflammatory molecular functions including IL-8, Toll-like receptors, and chemokine/cytokine activity (Table 2). The top biological pathways are presented in (Table 3) and include TP53 transcription regulation, activation of Ima kinases, and matrix metalloproteinases. DEGs derived from comparisons of pristane-exposed lung tissues from IgG-treated mice and mice receiving the ALT-100 mAb
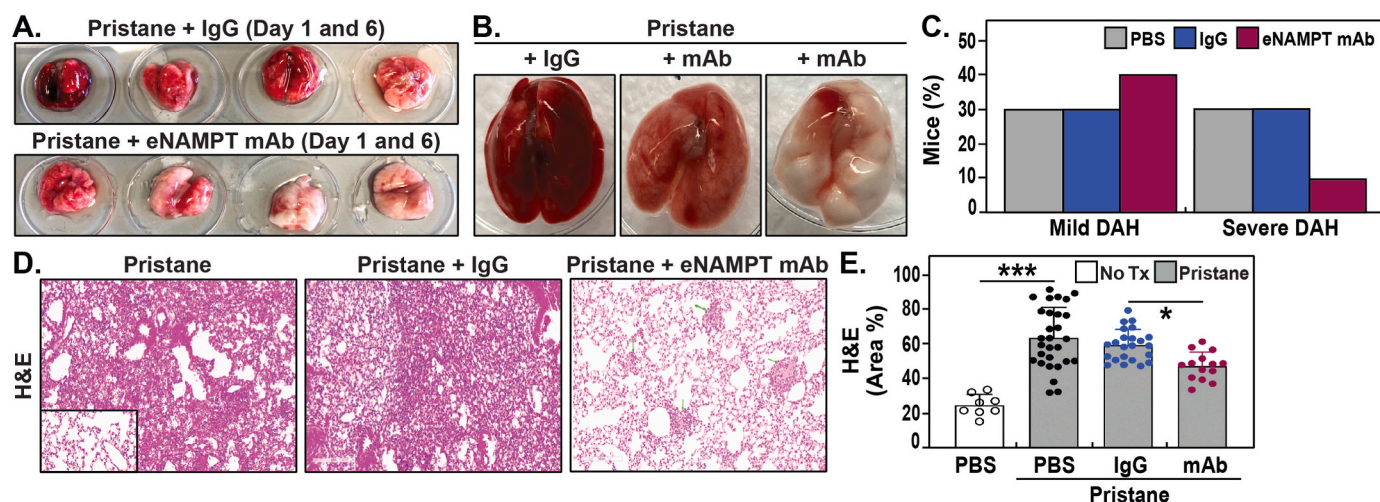
Fig. 3. The eNAMPT-neutralizing mAb reduces pristane-induced murine vasculitis and alveolar hemorrhage. A/B. Alveolar hemorrhage was absent in control mice that were not exposed to pristane challenge. All pristane-exposed mice receiving either PBS or IgG (controls) survived to Day 10 and exhibited varying degrees of alveolar hemorrhage (mild to severe) by gross whole lung pathology. Representative lung samples are depicted. In contrast, mice receiving the eNAMPT-neutralizing ALT-100 mAb (1 mg/kg) beginning on Day 1 showed substantial reduction in the severity of DAH by gross examination compared with PBS or IgG mice. **C.** Quantification of the extent of lung involvement with alveolar hemorrhage demonstrated similar severity in both the PBS- and IgG-treated pristane-challenged groups with each groups exhibiting comparable (30%) incidence of mild DAH and severe DAH. In contrast, only 10% of ALT-100 mAb-treated mice exhibited evidence of severe lung hemorrhage compared to 30% of PBS- or IgG-challenged mice. **D/E.** Histologic examination of pristane-induced lung inflammatory injury by H&E staining (four 20X fields) was examined in randomly selected areas on the H&E sections for each mouse and representative histology images are presented. These studies revealed dramatic immune cell and leukocyte infiltration in perivascular area which was similar in both PBS- and IgG-treated mice but significantly reduced in mice treated with the ALT-100 mAb, verified by Image J quantification of randomly selected H&E areas.

identified 447 DEGs (FDR <0.1, FC 2.0), with 57 upregulated and 390 down-regulated genes with the top DEGs depicted in a heat map (Fig. 5D). We next created a protein-protein interaction network for the ALT-100-influenced DEGs using the STRING-based interactome (Fig. 5E). This analysis identified six relevant groups of biological-related nodes with Groups #1-#4 predominantly inflammatory in nature. These nodes included TNF, IFN, NF-kappa-B and STAT signaling proteins (#1), Interleukin-1 inflammatory signaling and IL-1 receptor antagonist proteins (#2), matrix degradation and metalloproteinases, IL-6, Socs3 negative regulatory proteins and Jak/STAT pathway cytokines (#3), and chemotactic/inflammatory cytokines (#4). The Group #5 node was comprised of centromere and kinetochore mitotic-related proteins and Group #6 node contained cell cycle control and G1/S-specific-related proteins.

The top KEGG prioritized pathways generated by ALT-100 mAb-influenced genes from pristane-challenged mice included rheumatoid arthritis-related pathways, cytokine/cytokine receptor signaling, chemokine signaling, IL-17 signaling, p53 signaling, complement/coagulation cascades and TNFα/Toll-like receptor signaling (Table 4). Together these results are highly consistent with a critical role for the eNAMPT/TLR4 signaling pathway in pristane activation of evolutionarily-conserved inflammatory cascades that contribute to the severity of lung vasculitis and DAH pathobiology.

4. Discussion

Lupus vasculitis occurs in approximately 50% of SLE patients [48] affecting the multiple tissues including the skin (butterfly rash), heart, kidney and lung. Life-threatening lupus vasculitis most commonly seen with active lupus nephritis with diffuse alveolar hemorrhage (DAH) a severe complication affecting ~5% of SLE patients. DAH, often the initial presenting symptom of SLE, is variably treated with high dose corticosteroids, plasmapheresis, cyclophosphamide, rituximab, or mycophenolate mofetil, however, the paucity of randomized controlled trials specific for lupus vasculitis renders selection of therapeutic as arbitrary. Safe, effective treatments for lupus vasculitis and DAH remains an important unmet need in SLE.

The pathogenesis of SLE lung vasculitis is poorly understood but involves complex interactions between the vascular endothelium, inflammatory cells, cytokines, autoantibodies, and immune complexes that result in sterile inflammation, increased vascular permeability, complement/coagulation cascade activation, and leukocyte infiltration into vessels. DAMPs are chemically heterogeneous host-derived molecules that are rapidly released into the extracellular space from damaged extracellular matrices or dying cells under conditions of cellular/organ activation, stress, or injury [49,50]. In the absence of infection, DAMPs potently incite a sterile inflammatory response signal and immune responses via ligation of pattern-recognition receptors (PRRs) which include the Toll-like receptors and cytosolic Nod-like receptors, culminating in nuclear factor κB (NF-κB) activation and pro-inflammatory cytokine secretion. An increasing number of DAMPs have been linked to sterile inflammation and promotion of the maturation/activation of diverse immune cells and production of pro-inflammatory cytokine, events implicated in the pathogenesis of auto-immune diseases including rheumatoid arthritis (RA), SLE, psoriatic arthritis, and systemic sclerosis or scleroderma [51]. Continuous DAMP exposure has been linked the loss of tolerance to self-antigens in these diseases. SLE patients have impaired clearance of apoptotic debris which facilitates extracellular release of HMGB1 and other DAMPs whose activity is implicated in multiple disease phenotypes in SLE, including lupus nephritis and neuropsychiatric lupus. Understanding the mechanisms of sterile inflammation triggered by DAMPs is important in order to generate novel therapeutic auto-immune disease therapeutic strategies that target these molecules. For example, targeting DAMPs with nucleic acid scavengers has been suggested as a SLE therapeutic approach to reduce nucleic acid autoantibodies [52].

We previously utilized multi-species preclinical inflammatory models coupled with genomic–intensive approaches [53,54] to identify eNAMPT as a potent proinflammatory cytozyme that regulates nicotinamide adenine dinucleotide (NAD) biosynthesis [55,56] and serves as a novel innate immunity-activating DAMP [12]. Importantly, we have convincingly demonstrated eNAMPT's DAMP activity stems from high affinity ligation of the PRR, Toll-like receptor 4 (TLR4), to elicit robust NFkB-mediated signaling [12]. In humans and preclinical models,
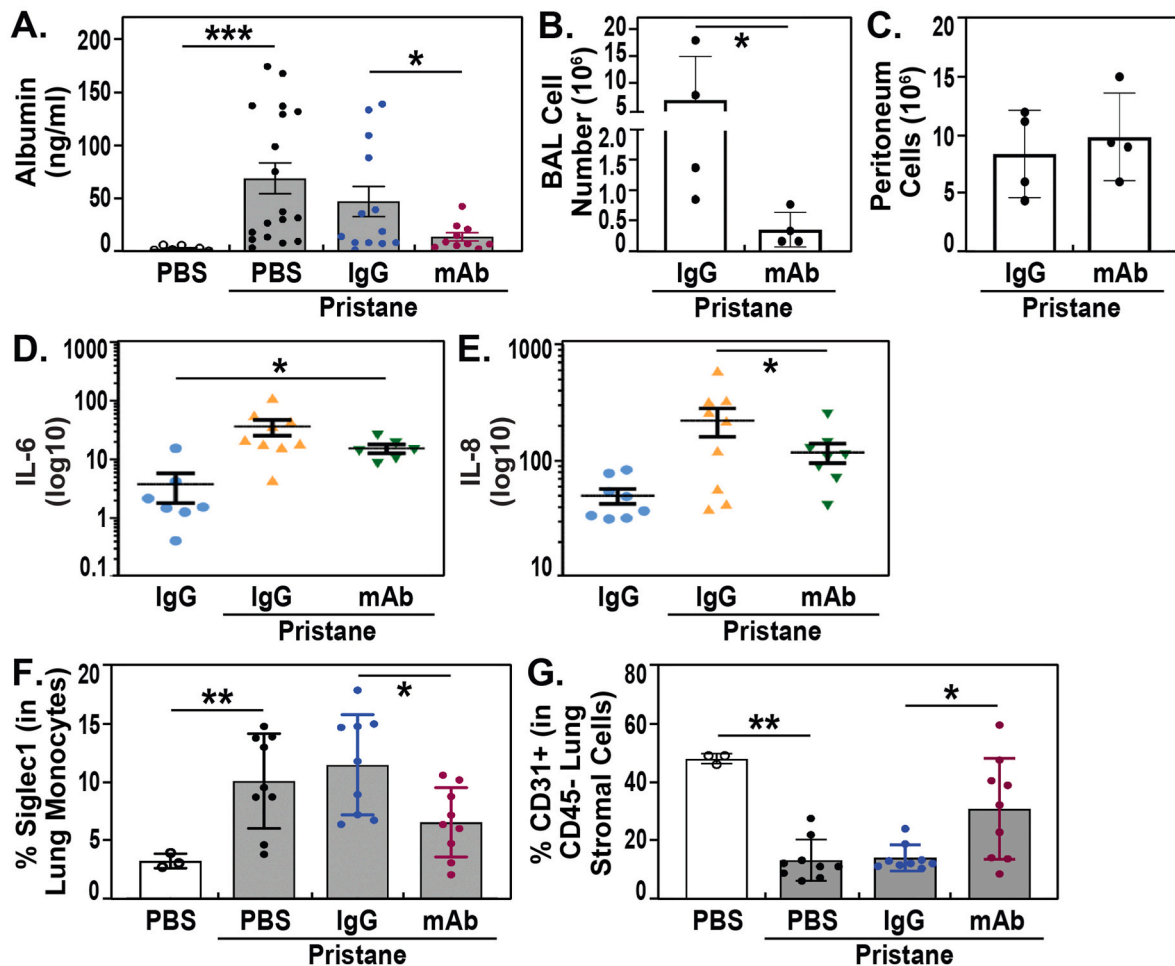
Fig. 4. eNAMPT neutralization reduces pristane-induced murine lung inflammation. A/B. Pristane-exposed mice exhibited significant inflammatory injury reflected by several BAL, tissue and blood indices. For example, BAL protein levels and numbers of BAL inflammatory cells at Day 10 were significantly increased in pristane-exposed, IgG-treated mice compared to unexposed controls but significantly reduced in mice receiving the ALT-100 mAb. **C.** In contrast to BAL results, quantification of peritoneal lavage cells from pristane-challenged mice showed no significant effect of ALT-100 mAb compared to IgG control mice. **D/E.** Levels of proinflammatory cytokines IL-6 and IL-8 were observed in pristane-exposed mice compared to control mice. Consistent with the inflammation-reducing capacity for the ALT-100 mAb and similar to the reductions in plasma levels of eNAMPT (Fig. 2B), reductions in IL-6 and IL-8 were observed in ALT-100 mAb-treated mice. **F/G.** Inflammatory cell subsets in pristane-exposed lungs were examined by flow cytometry. Significant accumulation of Siglec 1-positive CD11b + Ly6C + monocytes in the lung was observed whereas CD45⁻CD31⁺ vascular endothelial cells were significantly reduced by pristane exposure. ALT-100 mAb-treated mice showed normalization of these cellular inflammatory parameters with reduced numbers of Siglec1-positive CD11b + Ly6C + monocytes and increased numbers of lung endothelial cells compared to pristane only or IgG-treated mice.

eNAMPT is readily found within areas of sterile inflammation, such as the lungs and blood, with eNAMPT secretion augmented in response to hypoxia, severe bacterial and viral infections, trauma, radiation, and mechanical stress [23,31,38,57,58]. The current study confirms prior studies demonstrating increased circulating eNAMPT levels in patients with SLE [59,60] with SLE study subjects exhibiting both elevated eNAMPT protein and mRNA expression in blood. Pristane-exposed mice demonstrated similar increases in plasma eNAMPT and lung tissue NAMPT expression in a murine model of SLE vasculitis. Studies utilizing the eNAMPT-neutralizing mAb confirmed the involvement of eNAMPT/TLR4 inflammatory cascade activation in SLE-associated lung vasculitis with marked reductions in pristane-induced alveolar hemorrhage, inflammatory lung injury, leukocyte infiltration and preservation of vascular barrier integrity. Activation of the eNAMPT/TLR4 pathway in response to pristane-induced vasculitis is intimately involved in the evoked increases in circulating inflammatory cytokines, and profound loss of lung vascular barrier integrity, events directly linked to SLE mortality [35,61–63].

The precise cellular source of secreted eNAMPT is incompletely understood but is presumed to be highly stimulus- and organ-specific.

Previous localizing studies of acute inflammatory lung injury revealed robust spatially-localized NAMPT expression in lung endothelium, epithelium as well as in resident and infiltrating leukocytes [35]. Similar studies in a rat model of hypoxia/sugen-induced pulmonary hypertension confirmed enhanced NAMPT expression in lung endothelial cells (EC) [35]. Utilizing EC-specific conditional *NAMPT* KO mice, we showed the unequivocal involvement of EC-secreted eNAMPT in driving lung injury severity in both preclinical ARDS and PH models [25,57]. These studies strongly validate the viability of EC-derived eNAMPT as a SLE therapeutic target in lupus vasculitis/DAH and underscore the capacity of an eNAMPT-neutralizing biologic therapy to directly address the unmet need for novel strategies that improve lupus vasculitis mortality. The utility of the eNAMPT-neutralizing mAb in lupus vasculitis is supported by recently published studies detailing the efficacy of eNAMPT/TLR4 pathway targeting in preclinical ARDS [31,34,57,58], pulmonary hypertension [25], radiation pneumonitis [23], radiation fibrosis [38], and prostate cancer [64,65].

We employed FACS cell sorting of pristane-exposed murine lungs to assess the inflammatory components in the SLE model influenced by ALT-100 mAb. Our prior studies highlighted eNAMPT as a PMN

(caption on next page)

Fig. 5. eNAMPT neutralization reduces pristane-induced NFkB inflammatory signaling and differential gene/pathway dysregulation. A/B. Lung tissue homogenates were obtained from IgG-treated and eNAMPT ALT-100 mAb-treated pristane-exposed mice (n = 6/group) and compared to unexposed control mice (n = 4). Western blotting studies revealed striking increases in NFκB phosphorylation/total NFκB levels in lung homogenates obtained from pristane-exposed mice (lanes 5–8) compared to controls (first 4 lanes). Mice receiving the eNAMPT-neutralizing ALT-100 mAb demonstrated near abolishment of the increased levels of phosphorylated NFκB in pristane-exposed mice (lanes 9–12). These studies indicate that the eNAMPT/TLR4 inflammatory signaling pathway is a major driver of the innate immunity response to pristane challenge. A/C. Western blotting studies were also conducted in lung homogenates to examine DOCK1 protein immunoreactivity, a critical regulator of vascular barrier integrity [47]. These studies identified significant reductions in DOCK1 expression, which were restored in mice receiving the eNAMPT-neutralizing ALT-100 mAb. D. RNA sequencing data from pristane-exposed lung tissues (Day 10) from IgG- and ALT-100 mAb-treated mice was analyzed and yielded 447 DEGs (FDR <0.1, FC 2.0), with the top DEGs depicted in the heat map shown, 57 upregulated genes shown in green and 390 down-regulated genes shown in red. E. The STRING Functional protein network depicted shows the interaction of DEGs influenced by ALT-100 mAb treatment in mice exposed to pristane. The edges represent protein-protein associations, line color indicates the evidence the type of interaction (green-gene neighborhood, red-gene fusion, blue-co-occurrence, black-co-expression). The confidence interaction score is 0.15. Six relevant groups of biological-related nodes were identified as detailed in the Results/Discussion. **Group #1-** Genes involved in TNF, IFN, NF-kappa-B and STAT signaling. **Group #2-** Genes involved in Interleukin-1 inflammatory signaling and includes the IL-1 receptor antagonist which inhibits IL-1β by binding to its receptor to prevent its association with IL-1RAP for signaling. **Group #3-** Genes involved in matrix degradation with metalloproteinases which degrade fibronectin, collagens Il6, Socs3 negative reg, and cytokines involved in the Jak/STAT pathway. **Group #4-** Genes involved in chemotactic/and inflammatory pathways. **Group #5-** Genes involved in centromere and kinetochore mitotic-related proteins. **Group #6-** Genes involved in cell cycle control and G1/S-specific related proteins.

Table 2
Top Gene ontology "molecular function" terms in pristane-exposed lupus mice.

GO term ID	Term Description	Strength	False Discovery Rate
GO:0019959	Interleukin-8 binding	1.61	2.09E-02
GO:0035662	Toll-like receptor 4 binding	1.38	4.55E-02
GO:0045236	CXCR chemokine receptor binding	1.27	7.20E-04
GO:0050786	RAGE receptor binding	1.25	1.68E-02
GO:0008009	Chemokine activity	1.17	1.63E-09
GO:0004875	Complement receptor activity	1.09	4.12E-02
GO:0035325	Toll-like receptor binding	1.06	4.90E-02
GO:0019956	Chemokine binding	1	7.30E-04
GO:0016493	C–C chemokine receptor activity	1	7.60E-03
GO:0001848	Complement binding	0.98	2.63E-02
GO:0005125	Cytokine activity	0.77	1.89E-10
GO:0004896	Cytokine receptor activity	0.68	5.20E-03
GO:0008201	Heparin binding	0.55	1.45E-02

Table 3
Top dysregulated pathways in pristane-exposed lupus mice.

MMU pathway ID	Term Description	Strength	False Discovery Rate	Source
2980767	Activation of NIMA Kinases NEK9, NEK6, NEK7	1.51	1.80E-03	Reactome
69478	G2/M DNA replication checkpoint	1.38	2.28E-02	Reactome
6804116	TP53 Regulates Transcription of Genes Involved in G1 Cell Cycle Arrest	1.31	1.00E-03	Reactome
380108	Chemokine receptors bind chemokines	1.09	1.91E-09	Reactome
75205	Dissolution of Fibrin Clot	1.09	2.02E-02	Reactome
WP460	Blood clotting cascade	1.08	6.50E-04	Wiki
69273	Cyclin A/B1/B2 associated events during G2/M transition	1.07	3.80E-04	Reactome
WP441	Matrix metalloproteinases	1.05	7.59E-05	Wiki
5686938	Regulation of TLR by endogenous ligand	1.05	7.50E-03	Reactome
6791312	TP53 Regulates Transcription of Cell Cycle Genes	1.02	5.08E-05	Reactome
WP1253	Type II interferon signaling (IFNG)	0.95	7.20E-04	Wiki
04657	IL-17 signaling pathway	0.91	1.23E-08	KEGG
04610	Complement and coagulation cascades	0.9	1.27E-08	KEGG
140877	Formation of Fibrin Clot (Clotting Cascade)	0.87	4.10E-03	Reactome
mmu04115	p53 signaling pathway	0.8	1.30E-04	KEGG
mmu04060	Cytokine-cytokine receptor interaction	0.77	8.20E-16	KEGG

chemotaxin [34] and regulator of neutrophil maturation, activity, and life span as well as M2 macrophage polarization [66–68]. Shifting of pristane-treated macrophages to a M1 phenotype has been suggested to be critical in the development of pulmonary vasculitis [69,70]. Interestingly, Siglec 1 expression levels, widely used to assess inflammatory monocyte activation as precursors of resident tissue macrophages, were markedly increased in pristane-exposed mice and reduced in mice receiving ALT-100 mAb.

Our combined biochemical and genomic approaches further confirmed the key role for eNAMPT/TLR4 pathway activation in the development of lung vasculitis in pristane-exposed lung tissues with striking increases in NFkB activation which was significantly attenuated in mice receiving the ALT-100 mAb (Fig. 5). The significant reductions in DOCK1 expression observed in pristane-exposed mice were restored/ preserved in eNAMPT mAb-treated mice, a finding that provides insight into the eNAMPT/TLR4 signaling paradigm that produces severe vascular leakage and alveolar hemorrhage, given the now appreciated role of DOCK1 in preservation of vascular integrity [47]. Genomic studies of DEGs and signaling pathways influenced by ALT-100 mAb highlighted signaling pathways previously associated with multiple autoimmune disorders (cytokine/cytokine receptor, chemokine, IL-17, p53, and TNFα/Toll-like receptor, Table 4). The identification of highly significant DEGs in the complement/coagulation cascade (*Plaur-Urokinase plasminogen activator receptor, Serpine1-serine proteinase inhibitor*) is highly consistent with the known incidence of thrombotic manifestations in SLE patients even when compared with patients with other autoimmune disorders.

5. Conclusion

In summary, these human and preclinical studies are highly consistent with a critical role for the eNAMPT/TLR4 signaling pathway in activation of evolutionarily-conserved inflammatory cascades that contribute to the severity of lupus vasculitis and DAH pathobiology. Our results indicate that IP- and subcutaneously-delivered eNAMPT-neutralizing ALT-100 mAb, known to be an effective biologic therapeutic in preclinical ARDS [31,57,58] pulmonary hypertension [25], and radiation lung injury and fibrosis [23,38], may represent a novel approach to improve SLE-associated lung vasculitis. By dampening pro-inflammatory cytokine production, reducing immune cell infiltration into the lung, and attenuating lung vascular damage and permeability, the ALT-100 mAb may be a candidate for future studies designed to further characterize the therapeutic efficacy of eNAMPT-targeted

Table 4
Top Dysregulated KEGG Pathways in ALT-100 mAb-Treated Mice.

Pathway ID	Term Description	Strength	False Discovery Rate
mmu 04061	Viral protein interaction with cytokine and cytokine receptor	1.06	1.23E-10
mmu04060	Cytokine-cytokine receptor interaction	0.75	2.34E-10
mmu 04657	IL-17 signaling pathway	0.97	5.59E-08
mmu 04668	TNF signaling pathway	0.81	2.25E-05
mmu 04110	Cell cycle	0.77	4.58E-05
mmu 05323	Rheumatoid arthritis	0.85	5.45E-05
mmu 04610	Complement and coagulation cascades	0.82	8.70E-05
mmu 04062	Chemokine signaling pathway	0.66	0.0001
mmu04115	p53 signaling pathway	0.85	0.00039
mmu 04620	Toll-like receptor signaling pathway	0.75	0.0006
mmu 04623	Cytosolic DNA-sensing pathway	0.79	0.0055
mmu 04621	NOD-like receptor signaling pathway	0.54	0.0057
mmu 05166	Human T-cell leukemia virus 1 infection	0.5	0.0078
mmu 04064	NF-kappa B signaling pathway	0.65	0.0109
mmu 05160	Hepatitis C	0.55	0.0125
mmu 05206	MicroRNAs in cancer	0.5	0.0375
mmu 05161	Hepatitis B	0.49	0.04
mmu 05202	Transcriptional misregulation in cancer	0.46	0.04

biologics in SLE subjects.

Author contributions

Conceptualization – JGNG, GT, CJ, Data Curation - GT, SS, NGC, Formal analysis – JGNG, CJ, Funding acquisition – JGNG, CJ, Investigation - GT, DJW, JHS, VRH, DEL, JD, ENM, JMY, Methodology - GT, CLK, SS, NGC, Project administration – JGNG, CJ, MI, DJW, Resources – JGNG, CJ, Software - GT, NGC, Supervision – JGNG, SS, CJ, Validation – SS, CLK, Visualization – SMC, NGC, JHS, Writing-original draft – JGNG, GT, SMC, Writing-reviewing & editing – JGNG, GT, CT, CJ, NGC, CLK, SMC.

Declaration of competing interest

The authors declare the following financial interests/personal relationships which may be considered as potential competing interests: Joe G.N. Garcia, MD reports financial support and equipment, drugs, or supplies were provided by Aqualung Therapeutics, LLC. Joe G.N. Garcia, MD reports a relationship with Aqualung Therapeutics, LLC that includes: equity or stocks. Joe G.N. Garcia, MD has patent pending to Aqualung Therapeutics, LLC.

Data availability

Data will be made available on request.

Appendix A. Supplementary data

Supplementary data to this article can be found online at https://doi.org/10.1016/j.jtauto.2022.100181.

References

[1] C. Drenkard, S.S. Lim, Update on lupus epidemiology: advancing health disparities research through the study of minority populations, Curr. Opin. Rheumatol. 31 (2019) 689–696.
[2] J.R. Hannah, D.P. D'Cruz, Pulmonary complications of systemic lupus erythematosus, Semin. Respir. Crit. Care Med. 40 (2019) 227–234.
[3] O. Torre, S. Harari, Pleural and pulmonary involvement in systemic lupus erythematosus, Presse Med. 40 (2011) e19–e29.
[4] K. Tselios, M.B. Urowitz, Cardiovascular and pulmonary manifestations of systemic lupus erythematosus, Curr. Rheumatol. Rev. 13 (2017) 206–218.
[5] H. Zhuang, S. Han, P.Y. Lee, R. Khaybullin, S. Shumyak, L. Lu, et al., Pathogenesis of diffuse alveolar hemorrhage in murine lupus, Arthritis Rheumatol. 69 (2017) 1280–1293.
[6] N. Agmon-Levin, C. Selmi, The autoimmune side of heart and lung diseases, Clin. Rev. Allergy Immunol. 44 (2013) 1–5.
[7] H. Badsha, C.L. Teh, K.O. Kong, T.Y. Lian, H.H. Chng, Pulmonary hemorrhage in systemic lupus erythematosus, Semin. Arthritis Rheum. 33 (2004) 414–421.
[8] D.L. Kamen, C. Strange, Pulmonary manifestations of systemic lupus erythematosus, Clin. Chest Med. 31 (2010) 479–488.
[9] M.R. Zamora, M.L. Warner, R. Tuder, M.I. Schwarz, Diffuse alveolar hemorrhage and systemic lupus erythematosus. Clinical presentation, histology, survival, and outcome, Medicine (Baltim.) 76 (1997) 192–202.
[10] M.S. Park, Diffuse alveolar hemorrhage, Tuberc. Respir. Dis. 74 (2013) 151–162.
[11] G. Colombo, N. Clemente, A. Zito, C. Bracci, F.S. Colombo, S. Sangaletti, et al., Neutralization of extracellular NAMPT (nicotinamide phosphoribosyltransferase) ameliorates experimental murine colitis, J. Mol. Med. (Berl.) 98 (2020) 595–612.
[12] S.M. Camp, E. Ceco, C.L. Evenoski, S.M. Danilov, T. Zhou, E.T. Chiang, et al., Unique toll-like receptor 4 activation by NAMPT/PBEF induces NFkappaB signaling and inflammatory lung injury, Sci. Rep. 5 (2015), 13135.
[13] A. Manago, V. Audrito, F. Mazzola, L. Sorci, F. Gaudino, K. Gizzi, et al., Extracellular nicotinate phosphoribosyltransferase binds Toll like receptor 4 and mediates inflammation, Nat. Commun. 10 (2019) 4116.
[14] A.R. Moschen, A. Kaser, B. Enrich, B. Mosheimer, M. Theurl, H. Niederegger, et al., Visfatin, an adipocytokine with proinflammatory and immunomodulating properties, J. Immunol. 178 (2007) 1748–1758.
[15] N.E. Ramirez Cruz, C. Maldonado Bernal, M.L. Cuevas Uriostegui, J. Castanon, C. Lopez Macias, A. Isibasi, Toll-like receptors: dysregulation in vivo in patients with acute respiratory distress syndrome, Rev. Alerg. Mex. 51 (2004) 210–217.
[16] H. Lynn, X. Sun, N. Casanova, M. Gonzales-Garay, C. Bime, J.G.N. Garcia, Genomic and genetic approaches to deciphering acute respiratory distress syndrome risk and mortality, Antioxidants Redox Signal. 31 (2019) 1027–1052.
[17] X. Sun, B.L. Sun, A. Babicheva, R. Vandenpool, R.C. Oita, N. Casanova, et al., Direct eNAMPT involvement in pulmonary hypertension and vascular remodeling: transcriptional regulation by SOX and HIF2α, Am. J. Respir. Cell Mol. Biol. (2020). In press.
[18] C. Bime, S.M. Camp, N. Casanova, R.C. Oita, J. Ndukum, H. Lynn, et al., The acute respiratory distress syndrome biomarker pipeline: crippling gaps between discovery and clinical utility, Transl. Res. 226 (2020) 105–115.
[19] D.M. Adyshev, V.R. Elangovan, N. Moldobaeva, B. Mapes, X. Sun, J.G. Garcia, Mechanical stress induces pre-B-cell colony-enhancing factor/NAMPT expression via epigenetic regulation by miR-374a and miR-568 in human lung endothelium, Am. J. Respir. Cell Mol. Biol. 50 (2014) 409–418.
[20] C. Bime, N. Casanova, R.C. Oita, J. Ndukum, H. Lynn, S. M, Camp et al. Development of a biomarker mortality risk model in acute respiratory distress syndrome, Crit. Care 23 (2019) 410.
[21] D. Bojkova, K. Klann, B. Koch, M. Widera, D. Krause, S. Ciesek, et al., Proteomics of SARS-CoV-2-infected host cells reveals therapy targets, Nature 583 (2020) 469–472.
[22] V.R. Elangovan, S.M. Camp, G.T. Kelly, A.A. Desai, D. Adyshev, X. Sun, et al., Endotoxin- and mechanical stress-induced epigenetic changes in the regulation of the nicotinamide phosphoribosyltransferase promoter, Pulm. Circ. 6 (2016) 539–544.
[23] A.N. Garcia, N.G. Casanova, D.G. Valera, X. Sun, J.H. Song, C.L. Kempf, et al., Involvement of eNAMPT/TLR4 signaling in murine radiation pneumonitis: protection by eNAMPT neutralization, Transl. Res. 239 (2022) 44–57.
[24] H. Quijada, T. Bermudez, C.L. Kempf, D.G. Valera, A.N. Garcia, S.M. Camp, et al., Endothelial eNAMPT amplifies pre-clinical acute lung injury: efficacy of an eNAMPT-neutralising monoclonal antibody, Eur. Respir. J. 57 (2021).

[25] M. Ahmed, N. Zaghloul, P. Zimmerman, N.G. Casanova, X. Sun, J.H. Song, et al., Endothelial eNAMPT drives EndMT and preclinical PH: rescue by an eNAMPT-neutralizing mAb, Pulm. Circ. 11 (2021), 20458940211059712.

[26] V.R. Chowdhary, J.P. Grande, H.S. Luthra, C.S. David, Characterization of haemorrhagic pulmonary capillaritis: another manifestation of Pristane-induced lupus, Rheumatology 46 (2007) 1405–1410.

[27] P.A. Jarrot, E. Tellier, L. Plantureux, L. Crescence, S. Robert, C. Chareyre, et al., Neutrophil extracellular traps are associated with the pathogenesis of diffuse alveolar hemorrhage in murine lupus, J. Autoimmun. 100 (2019) 120–130.

[28] J.G. Garcia, K.L. Schaphorst, A.D. Verin, S. Vepa, C.E. Patterson, V. Natarajan, Diperoxovanadate alters endothelial cell focal contacts and barrier function: role of tyrosine phosphorylation, J. Appl. Physiol. 89 (2000) 2333–2343, 1985.

[29] S.Q. Ye, L.Q. Zhang, D. Adyshev, P.V. Usatyuk, A.N. Garcia, T.L. Lavoie, et al., Pre-B-cell-colony-enhancing factor is critically involved in thrombin-induced lung endothelial cell barrier dysregulation, Microvasc. Res. 70 (2005) 142–151.

[30] M.C. Hochberg, Updating the American College of Rheumatology revised criteria for the classification of systemic lupus erythematosus, Arthritis Rheum. 40 (1997) 1725.

[31] T. Bermudez, S. Sammani, J.H. Song, V.R. Hernon, C.L. Kempf, A.N. Garcia, et al., eNAMPT neutralization reduces preclinical ARDS severity via rectified NFkB and Akt/mTORC2 signaling, Sci. Rep. 12 (2022) 696.

[32] X. Peng, P.M. Hassoun, S. Sammani, B.J. McVerry, M.J. Burne, H. Rabb, et al., Protective effects of sphingosine 1-phosphate in murine endotoxin-induced inflammatory lung injury, Am. J. Respir. Crit. Care Med. 169 (2004) 1245–1251.

[33] M. Geraci-Erck, Immunohistochemistry research applications for animal tissue, NSH 32nd Symposium;Wokshop, vol. 82, 1–67.

[34] S.B. Hong, Y. Huang, L. Moreno-Vinasco, S. Sammani, J. Moitra, J.W. Barnard, et al., Essential role of pre-B-cell colony enhancing factor in ventilator-induced lung injury, Am. J. Respir. Crit. Care Med. 178 (2008) 605–617.

[35] S.Q. Ye, B.A. Simon, J.P. Maloney, A. Zambelli-Weiner, L. Gao, A. Grant, et al., Pre-B-cell colony-enhancing factor as a potential novel biomarker in acute lung injury, Am. J. Respir. Crit. Care Med. 171 (2005) 361–370.

[36] E.C. Jensen, Quantitative analysis of histological staining and fluorescence using ImageJ, Anat. Rec. 296 (2013) 378–381.

[37] R.C. Oita, S.M. Camp, W. Ma, E. Ceco, N. Harbeck, P. Singleton, et al., Novel mechanism for nicotinamide phosphoribosyltransferase inhibition of TNF-alpha-mediated apoptosis in human lung endothelial cells, Am. J. Respir. Cell Mol. Biol. 59 (2018) 36–44.

[38] A.N. Garcia, N.G. Casanova, C.L. Kempf, T. Bermudez, D.G. Valera, J.H. Song, et al., eNAMPT is a novel DAMP that contributes to the severity of radiation-induced lung fibrosis, Am. J. Respir. Cell Mol. Biol. Vol 66, Iss 5, pp 497–509, May 2022 (2022).

[39] A. Dobin, C.A. Davis, F. Schlesinger, J. Drenkow, C. Zaleski, S. Jha, et al., STAR: ultrafast universal RNA-seq aligner, Bioinformatics 29 (2013) 15–21.

[40] B. Li, C.N. Dewey, RSEM: accurate transcript quantification from RNA-Seq data with or without a reference genome, BMC Bioinf. 12 (2011) 323.

[41] P.J. Cock, C.J. Fields, N. Goto, M.L. Heuer, P.M. Rice, The Sanger FASTQ file format for sequences with quality scores, and the Solexa/Illumina FASTQ variants, Nucleic Acids Res. 38 (2010) 1767–1771.

[42] Y. Benjamini, Y. Hochberg, Controlling the false discovery rate: a practical and powerful approach to multiple testing, JR Statist. Soc. B 57 (1995) 289–300. Find this article online.

[43] A. Kamburov, U. Stelzl, H. Lehrach, R. Herwig, The ConsensusPathDB interaction database: 2013 update, Nucleic Acids Res. 41 (2013) D793–D800.

[44] D. Szklarczyk, J.H. Morris, H. Cook, M. Kuhn, S. Wyder, M. Simonovic, et al., The STRING database in 2017: quality-controlled protein-protein association networks, made broadly accessible, Nucleic Acids Res. 45 (2017) D362–D368.

[45] L. Bossaller, V.A. Rathinam, R. Bonegio, P.I. Chiang, P. Busto, A.R. Wespiser, et al., Overexpression of membrane-bound fas ligand (CD95L) exacerbates autoimmune disease and renal pathology in pristane-induced lupus, J. Immunol. 191 (2013) 2104–2114.

[46] G. Tumurkhuu, S. Chen, E.N. Montano, D. Ercan Laguna, G. De Los Santos, J.M. Yu, et al., Oxidative DNA damage accelerates skin inflammation in pristane-induced lupus model, Front. Immunol. 11 (2020), 554725.

[47] J.H. Song, J.B. Mascarenhas, S. Sammani, C.L. Kempf, H. Cai, S, M, Camp et al. TLR4 activation induces inflammatory vascular permeability via Dock1 targeting and NOX4 upregulation, Biochim Biophys Acta Mol Basis Dis. 1868 (12) (2022), 166562, https://doi.org/10.1016/j.bbadis.2022.166562. Epub 2022 Sep 27. PMID: 36179995.

[48] P. Leone, M. Prete, E. Malerba, A. Bray, N. Susca, G. Ingravallo, et al., Lupus vasculitis: an overview, Biomedicines 9 (2021).

[49] W. Jiang, G. Gilkeson, Sex Differences in monocytes and TLR4 associated immune responses; implications for systemic lupus erythematosus (SLE), J. Immunother. Appl. 1 (2014) 1.

[50] Y.W. Wu, W. Tang, J.P. Zuo, Toll-like receptors: potential targets for lupus treatment, Acta Pharmacol. Sin. 36 (2015) 1395–1407.

[51] K. Alvarez, G. Vasquez, Damage-associated molecular patterns and their role as initiators of inflammatory and auto-immune signals in systemic lupus erythematosus, Int. Rev. Immunol. 36 (2017) 259–270.

[52] L.B. Olson, N.I. Hunter, R.E. Rempel, B.A. Sullenger, Targeting DAMPs with nucleic acid scavengers to treat lupus, Transl Res 245 (2022) 30–40, https://doi.org/10.1016/j.trsl.2022.02.007.

[53] D.N. Grigoryev, S.F. Ma, R.A. Irizarry, S.Q. Ye, J. Quackenbush, J.G. Garcia, Orthologous gene-expression profiling in multi-species models: search for candidate genes, Genome Biol. 5 (2004) R34.

[54] B.A. Simon, R.B. Easley, D.N. Grigoryev, S.F. Ma, S.Q. Ye, T. Lavoie, et al., Microarray analysis of regional cellular responses to local mechanical stress in acute lung injury, Am. J. Physiol. 291 (2006) L851–L861.

[55] J.R. Revollo, A.A. Grimm, S. Imai, The regulation of nicotinamide adenine dinucleotide biosynthesis by Nampt/PBEF/visfatin in mammals, Curr. Opin. Gastroenterol. 23 (2007) 164–170.

[56] J.R. Revollo, A. Korner, K.F. Mills, A. Satoh, T. Wang, A. Garten, et al., Nampt/PBEF/Visfatin regulates insulin secretion in beta cells as a systemic NAD biosynthetic enzyme, Cell Metabol. 6 (2007) 363–375.

[57] H. Quijada, T. Bermudez, C.L. Kempf, D.G. Valera, A.N. Garcia, S.M. Camp, et al., Endothelial eNAMPT amplifies pre-clinical acute lung injury: efficacy of an eNAMPT-neutralising monoclonal antibody, Eur. Respir. J. 57 (2021), 2002536.

[58] S. Sammani, T. Bermudez, C.L. Kempf, J.H. Song, J.C. Fleming, V. Reyes Hernon, et al., eNAMPT neutralization preserves lung fluid balance and reduces acute renal injury in porcine sepsis/VILI-induced inflammatory lung injury, Front. Physiol. 13 (2022), 916159.

[59] C.P. Chung, A.G. Long, J.F. Solus, Y.H. Rho, A. Oeser, P. Raggi, et al., Adipocytokines in systemic lupus erythematosus: relationship to inflammation, insulin resistance and coronary atherosclerosis, Lupus 18 (2009) 799–806.

[60] M. Vadacca, D. Margiotta, A. Rigon, F. Cacciapaglia, G. Coppolino, A. Amoroso, et al., Adipokines and systemic lupus erythematosus: relationship with metabolic syndrome and cardiovascular disease risk factors, J. Rheumatol. 36 (2009) 295–297.

[61] E.K. Bajwa, P.D. Boyce, J.L. Januzzi, M.N. Gong, B.T. Thompson, D.C. Christiani, Biomarker evidence of myocardial cell injury is associated with mortality in acute respiratory distress syndrome, Crit. Care Med. 35 (2007) 2484–2490.

[62] E.K. Bajwa, C.L. Yu, M.N. Gong, B.T. Thompson, D.C. Christiani, Pre-B-cell colony-enhancing factor gene polymorphisms and risk of acute respiratory distress syndrome, Crit. Care Med. 35 (2007) 1290–1295.

[63] D.S. O'Mahony, B.J. Glavan, T.D. Holden, C. Fong, R.A. Black, G. Rona, et al., Inflammation and immune-related candidate gene associations with acute lung injury susceptibility and severity: a validation study, PLoS One 7 (2012), e51104.

[64] B.L. Sun, X. Sun, N. Casanova, A.N. Garcia, R. Oita, A.M. Algotar, et al., Role of secreted extracellular nicotinamide phosphoribosyltransferase (eNAMPT) in prostate cancer progression: novel biomarker and therapeutic target, EBioMedicine 61 (2020), 103059.

[65] B.L. Sun, L. Tang, X. Sun, A.N. Garcia, S.M. Camp, E. Posadas, et al., A humanized monoclonal antibody targeting extracellular nicotinamide phosphoribosyltransferase prevents aggressive prostate cancer progression, Pharmaceuticals 14 (2021).

[66] V. Audrito, S. Serra, D. Brusa, F. Mazzola, F. Arruga, T. Vaisitti, et al., Extracellular nicotinamide phosphoribosyltransferase (NAMPT) promotes M2 macrophage polarization in chronic lymphocytic leukemia, Blood 125 (2015) 111–123.

[67] S.H. Jia, Y. Li, J. Parodo, A. Kapus, L. Fan, O.D. Rotstein, et al., Pre-B cell colony-enhancing factor inhibits neutrophil apoptosis in experimental inflammation and clinical sepsis, J. Clin. Invest. 113 (2004) 1318–1327.

[68] J. Skokowa, D. Lan, B.K. Thakur, F. Wang, K. Gupta, G. Cario, et al., NAMPT is essential for the G-CSF-induced myeloid differentiation via a NAD(+)-sirtuin-1-dependent pathway, Nat. Med. 15 (2009) 151–158.

[69] Q. Guo, J.R. Yaron, J.W. Wallen 3rd, K.F. Browder, R. Boyd, T.L. Olson, et al., PEGylated serp-1 markedly reduces pristane-induced experimental diffuse alveolar hemorrhage, altering uPAR distribution, and macrophage invasion, Front. Cardiovasc. Med. 8 (2021), 633212.

[70] F.S. Lemos, J.X. Pereira, V.F. Carvalho, E.S. Bernardes, R. Chammas, T.M. Pereira, et al., Galectin-3 orchestrates the histology of mesentery and protects liver during lupus-like syndrome induced by pristane, Sci. Rep. 9 (2019), 14620.